MULTI-CHANNEL RESTORATION OF ELECTRON MICROGRAPHS

Michael Vrhel[†], *Benes L. Trus*[*]

[†]Biomedical Engineering and Instrumentation Program, National Center for Research Resources
National Institutes of Health, Bethesda, MD 20892-5766 USA

[*]Computational Bioscience and Engineering Laboratory, Division of Computer Research and Technology
National Institutes of Health, Bethesda, MD 20892-5624 USA

ABSTRACT

We introduce a projection based multi-channel restoration method which is useful in cases for which there is no *a priori* information about the input signal. The method is especially helpful in situations where a large number of specimens are later combined to achieve additional noise reduction. We describe the approach and discuss the problem of restoring electron micrographs. The method does require knowledge of the impulse response of the degradation. For this reason, the sensitivity of the approach to uncertainty in this degradation is investigated through simulation.

1. INTRODUCTION

In electron microscopy, there exists a trade off between image contrast and the amount the image is in focus. As the image is brought into focus, its contrast decreases. For this reason, high resolution electron micrographs are recorded with a significant amount of defocus. This results in a degradation that includes the complete loss of information at certain spatial frequencies. Because these spatial frequencies are a function of the defocus, it is advisable to record multiple images at varying degrees of defocus [12]. These images can then be combined using a multi-channel restoration method to obtain a single restored micrograph.

To keep from damaging the specimen, high resolution electron micrographs of biological macro-molecules are recorded at low electron doses. The use of a low electron dose produces an image with a low SNR, typically on the order of 0dB. In practice, the noise is reduced in a post-processing phase, in which a large number of images of identical specimens are combined. The specimens may be combined by correlation averaging [3], or by a 3-D reconstruction algorithm [2].

Since there exists the possibility for additional noise reduction, the restoration method should not distort the signal. Statistical based multi-channel deconvolution approaches such as Wiener filtering, or Bayesian methods require *a priori* information about the input signal which may be difficult to obtain in practice [4,5,6,7,17]. Without the correct signal statistics the signal estimate can be distorted [13]. This distortion is not acceptable for applications in which additional noise reduction is achieved by combining a large number of images.

An approach to the multi-channel deconvolution problem is proposed, which requires no *a priori* information about the input signal. The method is a multi-channel extension of the generalized sampling problem discussed in [14] and includes as a special case a current processing technique in electron microscopy [16]. The approach incorporates knowledge of the final reconstruction method which can include splines, wavelets, or display devices. In addition, unlike most classical formulations, the input signal is not required to be band-limited; it can be an arbitrary finite energy function. The method enforces a system projection constraint which produces less smoothing of the signal than the statistical based techniques, at the expense of less noise reduction. The projection constraint insures no loss of signal information if the input signal is included in the reconstruction space (e.g. the class of bandlimited functions). The residual in such a case will consist of only noise. The approach should be especially useful for those applications in which avoiding signal distortion is more important than noise reduction, or for those cases in which no *a priori* information is available.

2. PROJECTION BASED MULTI-CHANNEL RESTORATION

Mathematically, the recording process for an N-channel system can be represented by

$$r_i(k,j) = \langle \varphi_i(x-k, y-j), s(x,y) \rangle + n_i(k,j) \qquad i = 1,.....N$$

where $r_i(k,j)$ is the recorded data for channel i, $n_i(k,j)$ is additive noise, $s(x,y)$ is the continuous input, and $\varphi_i(-x,-y)$ is the impulse response in the ith channel. Figure 1 contains a diagram of a two channel system, where $q_i(k,j)$ are digital

filters to be designed, and $\varphi_o(x,y)$ defines the output signal subspace

$$V_o = \left\{ h(x,y) = \sum_j \sum_k \varphi_o(x-k, y-j)\, p(k,j) \mid p(k,j) \in l_2 \right\}.$$

The problem is to design the filters $q_i(k,j)\ i = 1,.....N$, using no *a priori* signal information, such that the signal is not distorted. With these requirements, designing the system to act as a projector becomes desirable. Specifically, if the system is a projection operator, then given that the input $s(x,y)$ satisfies $s(x,y) \in V_o$ the output $f(x,y)$ will be a perfect reconstruction of the input signal. If the input $s(x,y)$ is not contained in V_o, then the best solution, in the least squares sense, is the orthogonal projection of $s(x,y)$ onto V_o. Since $s(x,y)$ is not directly available (nor is any *a priori* information about the signal), the least squares solution is difficult to obtain when $s(x,y) \notin V_o$. In this case, the system provides, as an estimate, the projection of $s(x,y)$ onto V_o orthogonal to a subspace defined by the input impulse responses.

It can be shown that the filters

$$Q_i(u,v) = \frac{W_i(u,v)\overline{A}_{oi}(u,v)}{\sum_{j=1}^{N} W_j(u,v)\left|A_{oj}(u,v)\right|^2} \qquad (1)$$

give rise to all projection solutions, where $Q_i(u,v)$ is the Fourier transform of $q_i(j,k)$ and

$$A_{oi}(u,v) = \sum_j \sum_k \Phi_o(u-k, v-j)\, \overline{\Phi}_i(u-k, v-j)$$

is the spectral input-output correlation function with $\Phi_i(u,v)$ the Fourier transform of $\varphi_i(x,y)$, and $\overline{\Phi}$ the complex conjugation of Φ. The coefficients $W_i(u,v)$ in the above filters are weighting terms that provide degrees of freedom in the filter design while enforcing the overall system projection constraint. If $\varphi_o(x,y) = \mathrm{sinc}(x)\ \mathrm{sinc}(y)$ (separable sinc), then the above equation reduces to a common restoration approach in microscopy [16].

The subspace to which the projection is orthogonal is

$$V_q = \left\{ h(x) = \sum_j \sum_k \varphi_q(x-k, y-j)\, p(k,j) \mid p(k,j) \in l_2 \right\}$$

where

$$\varphi_q(x-k, y-j) = \sum_{i=1}^{N} \sum_m \sum_n q_i(k-m, j-n)\, \varphi_i(x-m, y-n)$$

can be considered the overall input impulse response of the system.

Ideally, the weights $W_i(u,v)$ should be selected to reduce the noise at the system output. The power spectrum of the noise after the summation of the output of the restoration filters is (assuming independent noise between the channels)

$$P_N(u,v) = \sum_{i=1}^{N} \left|Q(u,v)\right|^2 P_{n_i}(u,v)$$

where $P_{n_i}(u,v)$ is the noise power spectrum introduced in channel i. The goal is to select the weights such that $P_N(u,v)$ is minimized at each frequency. From the form of (1) is clear that if $W_i(u,v)\ \ i = 1,...,N$ was the optimal solution, then $\alpha W_i(u,v)$ would also be optimal. Therefore, the problem of minimizing $P_N(u,v)$ can be approached as minimize

$$\sum_{i=1}^{N} \left(\left|W_i(u,v)\right|^2 \right) \left|A_{oi}(u,v)\right|^2 P_{n_i}(u,v)$$

with respect to $W_i(u,v)\ \ i = 1,...,N$ subject to the constraint

$$\sum_{i=1}^{N} \left|W_i(u,v)\right|^2 P_{n_i}(u,v) = \kappa$$

where κ is a positive constant. Minimization leads to the optimal weights $W_i(u,v) = \dfrac{1}{P_{n_i}(u,v)}$.

3. ELECTRON MICROSCOPY BACKGROUND

For the electron microscopy application, the noise free Fourier transform of the recorded values is given by (cf. [12])

$$R_i(u,v) = H(u,v)F(u,v)\left(\delta(u,v) + \sin\left[\gamma_i(u,v)\right]\right) S(u,v)$$

where $S(u,v)$ is the Fourier transform of the input signal and $H(u,v)F(u,v)\left(\delta(u,v) + \sin\left[\gamma_i(u,v)\right]\right)$ is the frequency response of channel i, which is to be estimated; here amplitude contrast effects have been ignored. The $F(u,v)$ term is produced by the finite aperture size of the microscope. $H(u,v)$ is a low pass function which is produced by source coherence effects. The exact shape of $H(u,v)$ is difficult to determine and compensation is usually not made for its effect. A significant degradation that is corrected for is $\sin\left[\gamma_i(u,v)\right]$. This portion of the microscope response produces phase reversals and frequency nulls. For the ith channel $\gamma_i(u,v)$ is

$$\gamma_i(u,v) = \frac{2\pi}{\lambda}\left[\frac{C_s\left(u^2+v^2\right)^2 \lambda^4}{4} - \frac{\Delta f_i \left(u^2+v^2\right)\lambda^2}{2} \right]$$

where λ is the operating wavelength of the microscope, C_s is the spherical aberration of the objective lens, and Δf_i is the focal setting of the microscope for the ith channel. The quantity λ is determined by the voltage setting of the microscope and is known *a priori*. The spherical aberration is known *a priori* and is often provided by the microscope manufacturer. To estimate the shape of $\sin\left[\gamma_i(u,v)\right]\ \ i = 1,.....N$ it is necessary to determine the parameters Δf_i for $i = 1,.....N$ from the recorded data.

The first step in estimating the Δf_i is computing an estimate of the power spectrum of the recorded data which is denoted by $\left|R_i(u,v)\right|^2$. Since the term $\sin\left[\gamma_i(u,v)\right]$ is radially symmetric, the power spectrum estimate is radially averaged. Minima of the radially averaged function $\left|R_i(f)\right|^2$ will occur near the zero crossings of the function $\sin\left[\gamma_i(0,v)\right]$. The position of

the minima can be estimated using a wavelet based method, or by visual inspection of the diffraction pattern. Due to the extreme noise and the effects of $H(u,v)$, it is possible that only one or two minima are distinguishable. Once the null locations are estimated, an estimate of Δf_i is calculated using

$$\min_{\Delta f_i} \sum_{k=1}^{M} \left(\gamma_i(0, f_k) - \pi k\right)^2$$

where M and f_k are respectively the number of detectable extrema and their positions in the radial average. Cepstral based approaches are not useful for estimating the defocus, since the nulls of $\sin[\gamma_i(u,v)]$ are not equally spaced [1,10].

4. PRACTICAL ISSUES

If there is an area of the frequency spectrum for which no signal information is obtained, then the projection based approach can over amplify the noise. To avoid boosting the noise, a clipping operation may be performed on the restoration filters prior to their use. Mathematically this operation can be represented by

$$Q_{t_i}(u,v) = \begin{cases} \delta\, e^{j(\angle Q(u,v))} & Q_i(u,v) > \delta \\ Q_i(u,v) & \text{else} \end{cases}$$

where the parameter δ is determined by the level of noise. This is similar to the regularization of inverse filters as described in [9]. Interestingly, for the single channel case ($N = 1$) the filter $Q_{t_1}(u,v)$ with $\delta = 1.0$ is a commonly used restoration method in electron microscopy (assuming the only degradation being corrected is $\sin[\gamma_i(u,v)]$). This filter amounts to simply correcting the phase reversals which occur from the degradation $\sin[\gamma_1(u,v)]$.

The restoration method described required knowing the exact frequency response of the channel degradations. The degradations must be estimated from the recorded data. In the case of electron microscopy, the noise is such that there may be significant uncertainty in the estimate of the defocus parameters which define the channel responses. Therefore, we will look at the sensitivity of the restoration method to errors in this parameter.

5. SIMULATIONS

Sensitivity of restoration methods to uncertainty in blur estimates have been previously investigated but primarily for the single channel case and for camera blurs [11]. Here we perform a two channel simulation in which a test image shown in Fig. 3a is degraded by the terms $\delta(u,v) + \sin[\gamma_i(u,v)]$ with $\lambda = 3.69274$ pm, $C_s = 2$ mm, $\Delta f_1 = 1225$ nm, and $\Delta f_2 = 249$ nm. The radial profile of each channel frequency response is shown in Fig. 2. Estimates of the channel responses were computed from the location of the first zero. To simulate the uncertainty in this position, a series of restorations were performed in which the zero location was incorrectly estimated by up to 15 pixels in the frequency domain. A sampling rate of 4nm/pixel was simulated with 256x256 images. Noise was added to produce a signal to noise ratio of 0dB in each channel. The restored images were then ensemble averaged over 10 realizations to simulate the noise reduction achieved by combining multiple specimens. Degraded noisy images are shown in Fig. 3c-d. The frequency radial profiles of the restoration filters with optimum weights $W_i(u,v) = 1.0$ are shown in Fig. 2 when the correct zero locations were used. $\varphi_o(x,y)$ was the separable sinc (bandlimited reconstruction). The restoration using the filters in Fig 2 is shown in Fig. 3b. The mean square error was computed for each restoration and is shown in Table 1. The values shown were averaged over 10 simulations. A noise free case was also computed and is displayed in Table 2. As the level of noise increases, the sensitivity to errors in the estimated channel responses decreases. This is similar to the result described in [11]. Errors in estimating channel 1 produced larger errors than those in channel 2. From Figs. (2-3) it is clear that channel 2 provided high frequency information about the signal while channel 1 provided low frequency information. Since the input signal had more power at the lower frequencies the difference in the sensitivity to errors in channel 1 and 2 is expected.

6. CONCLUSION

Unlike classical statistical based methods, the projection based restoration preserves all of the signal information when the original signal is contained in the reconstruction space. In such a case, the residual will consist of noise only. This makes the method useful for applications such as electron microscopy in which noise is reduced in a post-processing stage. From the simulations it is clear that the sensitivity of the method to errors in the estimated channel responses decreases with decreasing SNR. Knowledge of this sensitivity will be useful in future work involving the multi-channel restoration of real microscopy data.

7. ACKNOWLEDGMENTS

We would like to thank Michael Unser for his helpful comments on this work. We would also like to thank Frank Booy for providing practical information on electron microscopy.

REFERENCES

[1] T. M. Cannon, "Blind Deconvolution of spatially invariant image blurs with phase," *IEEE Trans. Acoust., Speech, Signal Proc.*, Vol 24., pp. 58-63, Feb. 1976.

[2] H. Engelhardt, in: *Methods in Microbiology*, Vol. 20, Academic Press, London, 1988.
[3] J. Frank, A. Verschoor, and M. Boublik, "Computer Averaging of Electron Micrographs of 40S ribosomal subunits," *Science*, Vol. 214, pp. 1353-1355, 1981.
[4] N. P. Galatsanos and R. T. Chin, "Restoration of Color Images by Multichannel Kalman Filtering," *IEEE Trans. Signal Proc.*, Vol. 39, No. 10, pp. 2237-2252 Oct. 1991.
[5] N. P. Galatsanos and R. T. Chin, "Digital Restoration of Multichannel Images," *IEEE Trans. Acoust., Speech, Signal Proc.*, Vol. 37, No. 3, pp. 415-421, March 1989.
[6] X. Huang and J. Ximen, "Discussions on the Multiple-Input Maximum A-Posteriori Wave-Function Restoration Method in High Resolution Electron Microscopy," *J. Electon Micro. Tech.*, Vol. 17, pp. 344-350, 1991.
[7] B. R. Hunt and O. Kubler, "Karhunen-Loeve Multispectral Image Restoration, Part I: Theory," *IEEE Trans. Acoust., Speech, Signal Proc.*, Vol. 32, No. 3, pp. 592-599, June 1984.
[8] O. Rioul and M. Vetterli, "Wavelets and Signal Processing," *IEEE Signal Processing*, Vol. 8, No. 4, pp. 14-38, Oct. 1991.
[9] A. Rosenfeld and A. C. Kak, Digital Picture Processing, Academic Press, San Diego, 1982.
[10] A. E. Savakis and R. L. Easton, "Blur Identification Based on Higher Order Spectral Nulls," *International Symposium on Optics, Imaging, and Instrumentation*, SPIE Vol. 2302, July 24-29 1994.
[11] A. E. Savakis and H. J. Trussell, "On the Accuracy of PSF Representation in Image Restoration," *IEEE Trans. Image Proc.*, Vol. 2, No. 2, pp. 252-259, April 1993.
[12] W. O. Saxton, Computer Techniques for Image Processing in Electron Microscopy, Academic Press, New York, 1978.
[13] H. J. Trussell, M. I. Sezan, and D. Tran, "Sensitivity of Color LMMSE Restoration of Images to the Spectral Estimate," *IEEE Trans. Signal Proc.*, Vol. 39, No. 1, pp. 248-252, Jan. 1991.
[14] M. Unser and A. Aldroubi, "A General Sampling Theory for Non-ideal Acquisition Devices," *IEEE Trans. Signal Proc.*, Vol. 42, No. 11, pp. 2915-2925, Nov. 1994.
[16] N. Unwin, "Nicotinic Acetylcholine Receptor at 9 A Resolution," *J. Mol. Biol.*, Vol. 229, pp. 1101-1124, 1993.
[17] L. P. Yaroslavsky and H. J. Caulfield, "Deconvolution of Multiple Images of the Same Object," *Applied Optics*, Vol. 33, No. 11, pp. 2157-2162, April 1994.

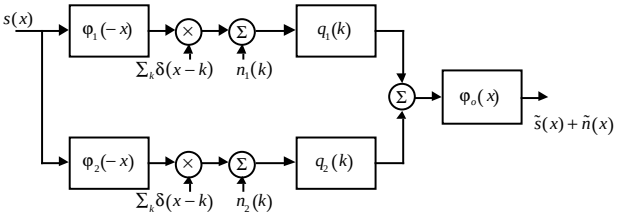

Figure 1: 2-channel system.

	-15	-10	5	0	5	10	15
-15	1227	770	487	445	700	1168	1868
-10	1228	791	474	434	709	1255	2042
-5	1226	734	473	432	727	1312	2174
0	1233	743	466	446	743	1354	2314
5	1256	769	511	444	752	1401	2406
10	1304	758	471	478	788	1447	2488
15	1321	767	482	449	784	1464	2566

Table 1: MSE for restorations at 0dB. The top row (-15,...,15) is the difference between the actual location of the first zero in the degradation and its estimate in terms of frequency samples for channel 1. The first column (-15,...,15) is the same but for channel 2.

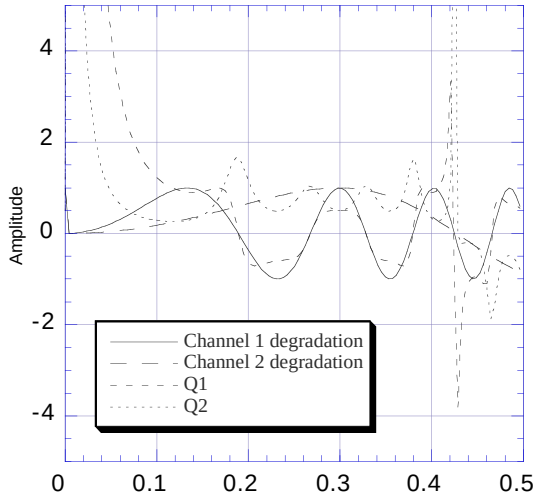

Figure 2: Radial average frequency plot of restoration filters Q1 and Q2 and the channel degradations

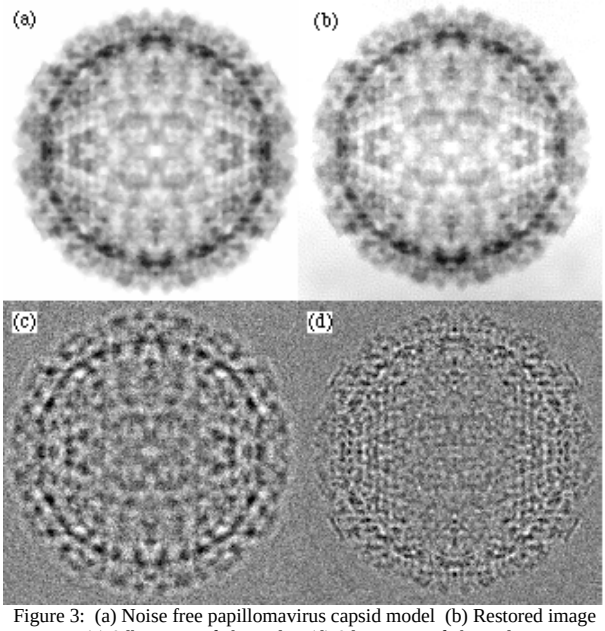

Figure 3: (a) Noise free papillomavirus capsid model (b) Restored image (c) 0db output of channel 1 (d) 0dB output of channel 2.

	-15	-10	-5	0	5	10	15
-15	1066	539	174	14.38	144	476	1028
-10	1061	544	158	5.71	144	537	1159
-5	1069	512	155	1.28	154	578	1270
0	1077	516	150	0.00	160	609	1372
5	1098	532	164	1.52	168	641	1451
10	1123	534	153	8.35	180	670	1518
15	1154	543	160	7.46	190	689	1578

Table 1: MSE for noise free restorations. The top row (-15,...,15) is the difference between the actual location of the first zero in the degradation and its estimate in terms of frequency samples for channel 1. The first column (-15,...,15) is the same but for channel 2.